CHEMISTRY OF MATERIALS

Article

pubs.acs.org/cm

Catechol-Modified Polyions in Layer-by-Layer Assembly to Enhance Stability and Sustain Release of Biomolecules: A Bioinspired Approach

Younjin Min and Paula T. Hammond*

Department of Chemical Engineering, Massachusetts Institute of Technology, Cambridge, Massachusetts 02139, United States

Supporting Information

ABSTRACT: Although layer−by−layer (LbL) assembly technique has been successfully used in various areas of nanobiotechnology, some LbL-assembled nanostructures have suffered from a lack of stability when they are exposed to certain changes in aqueous environments. In addition, the interlayer diffusion of polyelectrolytes throughout the film during assembly generally limits the control of film architecture and release characteristics. To overcome these limitations, we have utilized a strategy to conjugate catechol groups, largely present in mussel adhesive proteins, to branched poly(ethyleneimine) (BPEI) and poly(acrylic acid) (PAA). Only a fraction of amine or acid groups are modified with catechol groups, thereby preserving their charged nature for use in LbL assembly, while integrating the beneficial adhesive features of catechol groups into LbL films. The structure, physico−chemical properties, and stability of LbL films composing BPEI and PAA without and with catechol modifications were compared. The incorporation of catechol groups led to a doubling of the average film thickness and linear film growth. Upon exposure to PBS pH 7.4, the catechol-containing LbL films underwent far fewer changes in the degree of ionization and film thickness and exhibited stronger mechanical properties, indicative of their enhanced film stability. Finally, when LbL films with catechol modifications were used as physical barrier layers between radiolabeled ^{14}C−dextran sulfate (^{14}C−DS) and ^{3}H−heparin sulfate (^{3}H−HS), we observed two different release rates composed of an abrupt release from the surface of ^{3}H−HS, together with a sustained release from the underlying ^{14}C−DS. Overall, these films provide a bioinspired multifunctional platform for the systematic incorporation and assembly of biological therapeutics into controlled release films at physiological conditions for biomedical applications.

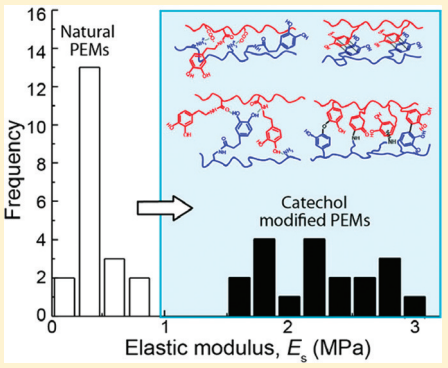

KEYWORDS: *polyelectrolytes, self-assembly, mussel adhesive protein, film stability, sustained release, cross-linking*

INTRODUCTION

Layer−by−layer (LbL) assembly technique has been proven to be an ideal method for preparation of multifunctional, nanostructured materials in various aspects of biomedical applications.[1−7] The preparation principles and procedures of the LbL assembly technique are quite simple, mainly relying on electrostatic interactions between oppositely charged polymers. Several reports on the use of LbL films for controlled release via hydrolytic[8] or enzymatic degradation[9] present the potential of these films as delivery systems; however, for certain systems that exhibit interdiffusion or exchange of components during assembly, LbL films can deliver some of their payload in a burst or bolus mode in the presence of external stimuli such as changes in pH or ionic strength. For example, several studies have reported that when polyelectrolyte multilayer films are built at low pH and/or low ionic strength and then transferred to a physiological medium at pH 7.4, the films are disrupted because of the change in charge balance, resulting in film destabilization and loss of materials from the substrate.[10−12]

Although a spatially organized LbL film has the potential to produce sequential release of more than one therapeutic component in drug delivery, its development has been challenging because of the phenomenon of interlayer diffusion. The tendency of polyelectrolytes to diffuse throughout LbL systems during the deposition process is believed to be due to a mismatch of charge density between oppositely charged polyelectrolytes,[13,14] and/or the enhanced mobility of polymers with low molecular weight or low charge densities or degree of ionization.[15,16] Thermal,[17] chemical,[18−20] and photo-cross-linking[21] routes have been employed in order to enhance the stability of LbL films in the use of long-term drug delivery applications in physiological media. However, when the incorporation of fragile and sensitive biomolecules such as proteins and plasmid DNA is involved, use of thermal, chemical, and photoreactive routes can be detrimental, as they can denature proteins and cleave DNA. While release of bioactive molecules and polyelectrolyte components can be instantly triggered by a wide variety of stimuli such as pH,[22,23] and ionic strength[12,24] by swelling and destabilizing the films; the fabrication of stable LbL films that can release their payload

Received: June 23, 2011
Revised: September 26, 2011
Published: December 1, 2011

in a controlled and prolonged manner using nondestructive routes still remains elusive. As such, there is an increasing need to develop alternative nondestructive strategies to enhance the stability of LbL films and eventually to achieve a long-term delivery of biomolecules. Here, we developed chemically and mechanically stable polyelectrolyte films inspired by the excellent adhesive properties of *Mytilus edulis* foot proteins (Mefps) in mussels.

These protein-based adhesives are found in the attachment apparatus of mussels called the byssus, which is a bundle of threads extending from within the shell of the mussels.[25] At least five Mefps have been identified, and all of them share a common distinguishing moiety, 3,4−dihydroxyphenyl (catechol) side chain that provides its unique adhesion-related properties.[26] Although the exact mechanism related to how catechol groups increase interfacial binding is not yet fully understood, it is well accepted that the catechols are particularly susceptible to oxidation under neutral to alkaline pH conditions (e.g., seawater), and the resultant oxidized forms are capable of many different types of chemical interactions, giving rise to a highly cross-linked three−dimensional matrix.[27] Of particular interest is the fact that, unlike disulfide, amine, and carboxylic chemistries, catechol reactions are orthogonal to protein and other biologic chemistries, and will not engage the functional groups of sensitive biologic drugs incorporated into multilayer films. Because of these strong interfacial binding properties and cross-linking capabilities, catechol groups have attracted some attention for film fabrication. For example, people have utilized catechol chemistry for modifying various types of flat substrates[28−30] and particles[31,32] and for increasing the mechanical properties of clay/polymer composites[33] as well as carbon nanotube fibers.[34] However, to the best of our knowledge, there have been no systematic studies about the effect of catechol functionalities on the stability of LbL films which, in turn, tune the release kinetics of encapsulated cargos from the films.

In this paper, we describe synthetic polyelectrolytes with catechol functionalities for use in LbL assembly, particularly in the hope of enhancing film stability and controlling the release times of biomolecules from the film. One of the most unique advantages of integrating catechol functionality is that oxidized catechol groups that form at pH 7.4 are cross-linked by the formation of various covalent bonds,[35−37] resulting in improving the film stability and slowing down the release kinetics. By partially conjugating catechol groups to both branched poly(ethyleneimine) (BPEI: cationic polymer) and poly(acrylic acid) (PAA: anionic polymer), we not only preserve the cationic and anionic characteristics of the polymers, but also incorporate additional attractive hydrogen bonding and $\pi-\pi$ stacking interactions into the system (see Figure 1a and Figure 7). These additional attractive interactions occur between opposite as well as like−charged polyelectrolytes, possibly compensating for charge mismatches, which is considered to be one cause of interdiffusion phenomena. Although electrostatic interactions still remain important, they are coupled with other types of attractive interactions, which are less sensitive to changes in aqueous environments (e.g., pH, ionic concentration) and therefore enhance film stability. All of these unique features of catechol groups can effectively reduce the mobility of polymer chains during LbL assembly (i.e., pH 5) as well as at physiological condition (pH 7.4) and in turn diminish the interdiffusion of polyelectrolytes. We also examined the effects of LbL films with catechol modifications as physical barrier layers on the release

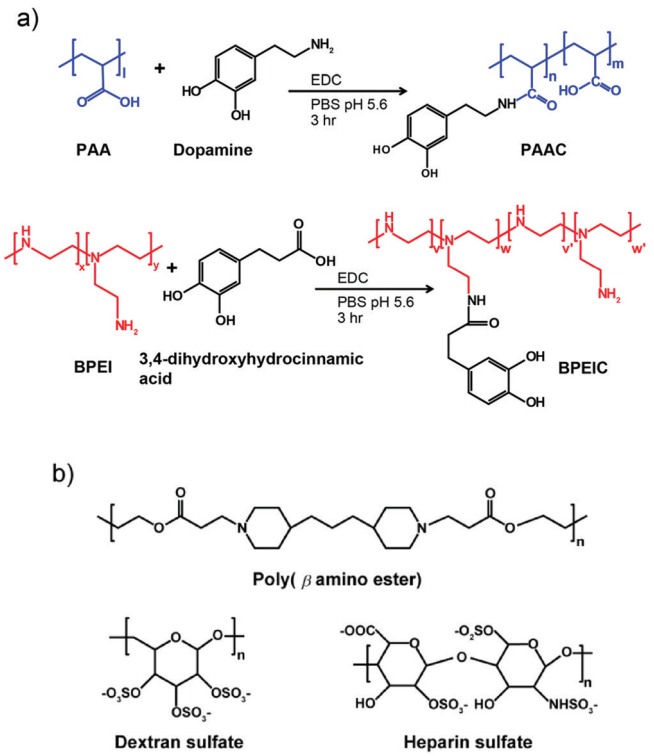

Figure 1. (a) Synthesis of catechol-modified poly(acrylic acid) (top) and branched polyethyleneimine (bottom); (b) chemical structures of degradable polymer and model drugs used in this study.

behavior of radiolabeled ^{14}C-dextran sulfate sodium salt (^{14}C-DS) and ^{3}H-heparin sulfate sodium salt (^{3}H-HS) from hydrolytically degradable anionic poly(β-amino ester) (Poly 1) LbL films (See Figure 1b).

EXPERIMENTAL SECTION

Materials. Poly(acrylic acid) (PAA) (M_w = 50 000, 25% aqueous solution), branched polyethyleneimine (BPEI) (M_w = 70 000, 30% aqueous solution), and linear polyethyleneimine (LPEI) (M_w = 25 000) were purchased from Polysciences Inc. (Warrington, PA). 3−hydroxytyramine (dopamine) hydrochloride, 3,4−dihydroxyhydrocinnamic acid, poly(sodium 4−styrenesulfonate) (SPS) (M_w = 100 000), phosphate buffered saline (PBS) powder (138 mM NaCl, 10 mM Na_2HPO_4 and 2.7 mM KCl), dimethyl sulfoxide (DMSO), hydrogen peroxide (30 wt % solution in water), and ammonium hydroxide (≥ 25 wt % solution in water) were purchased from Sigma Aldrich Co. (St Louis, MO). 1-Ethyl-3-(3-dimethylaminopropyl)carbodiimide hydrochloride (EDC) was purchased from Thermo Fisher Scientific Inc. (Rockford, IL). Poly(β-amino esters) (Poly 1) were synthesized according to previous literature.[38] Briefly, a solution of 4,4′−trimethylenedipiperidine (97%, Sigma) in anhydrous THF was added to 1,4-butanediol diacrylate monomer (99%, Aesar) dissolved in anhydrous THF (50 mL, Sigma). The reaction mixture was stirred for 66 h at 50 °C under nitrogen. After 66 h, the reaction was cooled to room temperature and precipitated in cold stirring hexanes. Polymers were collected and dried under vacuum prior to GPC analysis. The number average molecular weight of Poly(β-amino esters) was about 10 000. Microscope glass slides used for the deposition, hydrochloric acid (HCl) (1 M solution), and sodium hydroxide (NaOH) (1 M solution) were purchased from VWR (Edison, NJ). Fluorescamine was purchased from Invitrogen (Chicago, IL). Radiolabeled ^{14}C-dextran sulfate sodium salt (^{14}C-DS) (1.2 mCi/g, M_n = 8000) and ^{3}H-heparin sodium salt (^{3}H-HS) (1.5 mCi/mg, M_n = 6000) were obtained from American Radiolabeled Chemicals (St. Louis, CO). Standard regenerated cellulose (RC) dialysis membrane with 12,000−14,000 kDa molecular weight cutoff

dx.doi.org/10.1021/cm201801n | *Chem.Mater.* 2011, 23, 5349−5357

was purchased from Spectrum Laboratories Inc. (Rancho Dominguez, CA). Deionized water (>18.2 MΩ cm resistivity), obtained using a Milli-Q Plus system (Millipore, Bedford, MA), was used to make all solutions. Silicon wafers (test grade n−type) used for the deposition were purchased from Silicon Quest (Santa Clara, CA). All materials and solvents were used as received without further purification.

Synthesis of Catechol-Modified Polymers. Catechol-modified poly(acrylic acid) (PAAC) and branched polyethyleneimine (BPEIC) were synthesized in the presence of EDC, which is the most popular carbodiimide used for conjugating carboxylates and amines. Schematic illustrations of the synthesis procedures are provided in Figure 1. First, PAA and BPEI were dissolved in PBS buffer (Solution A). Specific amounts of EDC, dopamine, and 3,4-dihydroxyhydrocinnamic acid were then dissolved in PBS buffer (Solution B). The pH of each solution was adjusted to 5.6 by adding 1 M HCl or NaOH. Solution B was then added dropwise into Solution A, and the obtained solution was stirred for 3 h at room temperature. Unreacted chemicals and byproducts were removed by extensive dialysis for 3 days. The degree of substitution of catechol groups in PAAC was determined by ^{1}H-NMR resulting in 27.5 ± 0.8%. The catechol modification to BPEI was confirmed by ^{1}H NMR and quantified by fluorescamine assay with 28.2 ± 1.8% substitutions.

LbL Film Assembly. All substrates were first cleaned with ethanol and dried under a stream of nitrogen gas. An RCA cleaning solution (5:1:1 H_2O:H_2O_2 (30%):NH_3 (25%)) was then employed to clean the substrates at 75 °C for 5 min, rinsed copiously with deionized water, and dried under a stream of nitrogen gas. Next, the substrates were installed onto the holder and exposed to two minutes of oxygen plasma etch using a Harrick PDC−32G plasma cleaner (Harrick Plasma, Ithaca, NY). LbL films were constructed according to the alternate dipping method, using an automated Carl Zeiss HMS Series Programmable Slide Stainer. For film stability test of barrier layers, two different types of films were constructed as follows. First, a nondegradable base layer film of $(LPEI/X)_3$, where X = PAA or PAAC, was deposited by submerging the substrates in an LPEI solution at a concentration of 1 mg/mL in PBS buffer at pH 5 for 10 min, followed by a cascade rinse cycle consisting of three rinsing baths (30, 60, 60 s, respectively). Substrates were then submersed in either PAA or PAAC solution at a concentration of 1 mg/mL in PBS buffer at pH 5 for 10 min followed by the same cascade rinsing cycle; the entire process was then repeated three times. A barrier layer consisting of either $(BPEI/PAA)_n$ or $(BPEIC/PAAC)_n$, where n is the number of bilayers, was deposited on the existing $(LPEI/X)_3$ base layer by repeating the above procedures 5−30 times using either BPEI or BPEIC (1 mg/mL in PBS buffer, pH 5) as the polycationic species and either PAA or PAAC (1 mg/mL in PBS buffer, pH 5) as the polyanionic species. For sustained drug release experiments using two types of barrier layers, first a nondegradable base layer of $(LPEI/SPS)_{10}$ was deposited based on the procedures described above under same experimental conditions (PBS buffer, pH 5). Then, a degradable drug layer film of (Poly 1/^{14}C-DS)$_{20}$ was deposited on the existing $(LPEI/SPS)_{10}$ base layer by repeating the above procedures 20 times using Poly 1 (1 mg/mL in PBS buffer, pH 5) as the polycationic species and ^{14}C−DS (2 μCi/mL in PBS buffer, pH unadjusted) as the polyanionic species. Lastly, a nondegradable barrier layer of either $(BPEI/PAA)_{25}$ or $(BPEIC/PAAC)_{25}$ was deposited on top of drug and base layers by repeating the same procedures 25 times, generating the film architectures of either $(LPEI/SPS)_{10}$−(Poly 1/^{14}C-DS)$_{20}$−$(BPEI/PAA)_{25}$ or $(LPEI/SPS)_{10}$−(Poly 1/^{14}C-DS)$_{20}$−$(BPEIC/PAAC)_{25}$. For consecutive multiagent release experiments, the second degradable drug layer film of (Poly 1/^{3}H-HS)$_{20}$ was deposited on top of $(LPEI/SPS)_{10}$−(Poly 1/^{14}C-DS)$_{20}$−$(BPEIC/PAAC)_{25}$, resulting in a final film architecture of $(LPEI/SPS)_{10}$−(Poly 1/^{14}C-DS)$_{20}$−$(BPEIC/PAAC)_{25}$−(Poly 1/^{3}H-HS)$_{20}$. All experimental conditions for rinsing baths were kept the same as those in dipping baths (e.g., pH and same ionic strengths) to avoid any significant structural changes on the polyelectrolytes already adsorbed. After deposition, films were removed from the stainer, dried thoroughly, and kept in a desiccator until used, in order to lessen contact with air and humidity.

LbL Film Characterization. Film thickness was measured by Dektak 150 surface profiler (Veeco Instruments Inc., Santa Barbara, CA), and roughness of the LbL films was determined by using an atomic force microscope (Veeco Dimension 3100, Veeco Instruments Inc., Santa Barbara, CA). Fourier Transform Infrared Spectroscopy (FTIR) measurements were performed using a Nicolet 6700 Fourier Transform Infrared Spectrometer (Thermo Fisher Scientific Inc., Rockford, IL) with a Deuterated Triglycine Sulfate (DTGS) detector to verify film growth. The degree of ionization of PAA and PAAC in multilayer films was also estimated from FTIR spectra recorded in the dry state. Two distinct adsorption bands of the carboxylic acid functional groups of PAA and PAAC were considered: ν = 1565−1542 cm^{-1} (asymmetric stretching band of COO^-) and ν = 1710−1700 cm^{-1} (C═O stretching of COOH).[39,40] The deconvolution of these two peaks was done assuming a Gaussian distribution using OriginPro software. The corresponding band widths and areas at individual adsorption bands were quantified by assuming that the adsorption coefficient for both groups is approximately the same,[41] and that was used to estimate the degree of ionization of either PAA or PAAC, I_{COO-}, which is given by $(\nu_{COO-} \times 100)/(\nu_{COO-} + \nu_{COOH})$. The polymer components within the multilayers prepared for drug release experiments were also confirmed by the FTIR spectra.

Swelling Studies. The thickness changes of $(LPEI/PAA)_3$−$(BPEI/PAA)_{25}$ and $(LPEI/PAAC)_3$−$(BPEIC/PAAC)_{25}$ films were detected by the ex- and in−situ Ellipsometry (J.A. Woollam, Lincoln, NE) at room temperature. In situ measurements were conducted through a custom-made quartz cell with 70° windows (Hellma USA, Inc.). Data were collected between 300 and 1200 nm and analyzed using J.A. Woollam WVASE32 software, fitted with a Cauchy model, which assumes the real part of the refractive index, $n(\lambda)$ as a function of wavelength λ. The change in film thickness (Δd) between an as-prepared film and the film after being swollen (fully hydrated in PBS pH 7.4) is defined as:

$$\%\Delta d = \frac{(d_{\text{after swollen}} - d_{\text{as-prepared}})100}{d_{\text{as-prepared}}} \quad (1)$$

where $d_{\text{as-prepared}}$ is the dry thickness of an as-prepared film and $d_{\text{after swollen}}$ is the film thickness obtained in dry condition after the film was fully hydrated during in−situ swelling experiments. The simultaneous change in the degree of ionization (ΔI_{COO-}) was determined by quantifying and comparing the band intensities of COO^- peaks before and after being swollen states using the equation below:

$$\%\Delta I_{COO-} = \frac{(I_{COO-(\text{after swollen})} - I_{COO-(\text{as-prepared})})100}{I_{COO-(\text{as-prepared})}} \quad (2)$$

where $I_{COO-(\text{as-prepared})}$ is the relative mole number of COO^- groups per polymer chain in PAA or PAAC in an as-prepared film, and $I_{COO-(\text{after swollen})}$ is the relative mole number of COO^- groups per polymer chain after the film was fully hydrated.

Mechanical Testing of LbL Films. Mechanical properties of $(LPEI/PAA)_3$−$(BPEI/PAA)_{25}$ and $(LPEI/PAAC)_3$−$(BPEIC/PAAC)_{25}$ films were acquired in PBS pH 7.4 at 20 °C on a commercial scanning probe microscope (Molecular Force Probe 3D (MFP-3D), Asylum Research, Inc., Santa Barbara, CA). Unsharpened silicon nitride cantilevers of nominal probe radius $R_{tip} \approx 20$ nm (MCLT, Veeco Metrology Group, Sunnyvale, CA) were used to obtain the continuous force-displacement responses of the polyelectrolyte multiplayers (PEMs) in fluid. Prior to indentation, the actual spring constant k_c of each cantilever was determined experimentally as 178 ± 6 pN/nm. Nanoindentation was performed for at least 80 positions at a rate of 500 nm/s in an acoustic isolation enclosure. Indentation force-displacement responses were analyzed in IGOR Pro software (WaveMetrics, Lake Oswego, OR). An reduced elastic modulus, E_r, of the indented PEMs was then estimated by applying the Hertz contact model of the form[42] with a finite-thickness

correction:

$$F = \frac{16}{9} E_r R_{tip}^{1/2} \delta^{3/2} (1 + 1.133\chi + 1.283\chi^2 + 0.769\chi^3 + 0.0975\chi^4) \quad (3)$$

where F is the applied force, R_{tip} is the radius of curvature of the cantilevered probe, and δ is the depth of penetration into the sample surface. χ is defined as $(R_{tip}\delta/h)^{1/2}$ where h is the thickness of the PEMs in fluid. The obtained E_r was then used to estimate the elastic modulus of LbL films (E_s) based on the relationship:

$$E_r = \frac{E_s}{1 - \nu_s^2} + \frac{E_p}{1 - \nu_p^2} \quad (4)$$

where E_s, ν_s and E_p, ν_p are the Young's modulus and Poisson's ratio for the substrate material (LbL film) and the cantilevered probe material (Si_3N_4), respectively. Poisson's ratio was not measured experimentally, and was maintained fixed at a value of 0.33 and 0.50 for Si_3N_4 and the films, respectively, and E_p was assumed to be equal to 310 GPa.

Release Studies. Drug release experiments were performed by immersing each film in 14 mL of PBS buffer at pH 7.4 and 37 ± 0.5 °C. A 1 mL sample was extracted at the time points indicated in Figure 6 and analyzed by adding 5 mL of ScintiSafe Plus 50% (Thermo Fisher Scientific Inc., Rockford, IL) before measurement. Raw data (disintegrations per min per ml, DPM/ml) were converted to μg/mL ^{14}C-DS and ^{3}H-HS by using the conversion factor 2.2 × 10^6 DPM = 1 μCi. The total released amounts of ^{14}C-DS and ^{3}H-HS from a single film were then calculated according to the following equation:

$$M_i = C_i V_i + (1\text{mL}) \sum_{j=1}^{i-1} C_j \quad (5)$$

where M_i (μg) is the total cumulative mass released from the film as of measurement i; C_i (μg/mL) is the concentration of sample i; V_i (ml) is the total volume of the destruction bath before measurement i; and $(1\text{ mL})\sum_{j=1}^{i-1} C_j$ is the total mass in previously extracted samples.

RESULTS AND DISCUSSION

Figure 2 shows the growth curves and roughness of $(LPEI/PAA)_3$–$(BPEI/PAA)_n$ and $(LPEI/PAAC)_3$–$(BPEIC/PAAC)_n$ films assembled at pH 5 in 1 mg/mL polymer concentration composed with PBS buffer. In the case of $(LPEI/PAA)_3$–$(BPEI/PAA)_n$, the overall growth curve appears to consist of an initial lag growth phase where thickness does not increase significantly, followed by a linear growth with an average bilayer thickness of ~20 nm. The surface becomes smooth (laterally homogeneous) after n = 10 with an increasing number of layers, resulting in a final roughness of ~2 nm when n = 30. In the case of $(LPEI/PAAC)_3$–$(BPEIC/PAAC)_n$ films, the overall growth curves clearly show linear growth even in the first few layers. Considering the mechanisms and origins of layer formation, at acidic pH conditions such as pH 5 in this particular case, LPEI is known to undergo extensive interdiffusion,[15] leading to rearrangements of chains on the surface and increased roughness in the first few deposition cycles.[13] For the LPEI/PAA versus LPEI/PAAC base layers used in the films, the introduction of additional secondary interactions may have decreased diffusion of polymer chains during the adsorption process, thus lowering polymer chain mobility in the base layers and thereby eliminating or greatly reducing the high roughness portion of the curve caused by LPEI interdiffusion. Following application of the respective base layers, both the BPEI/PAA films (Figure 2a) and the catechol-modified

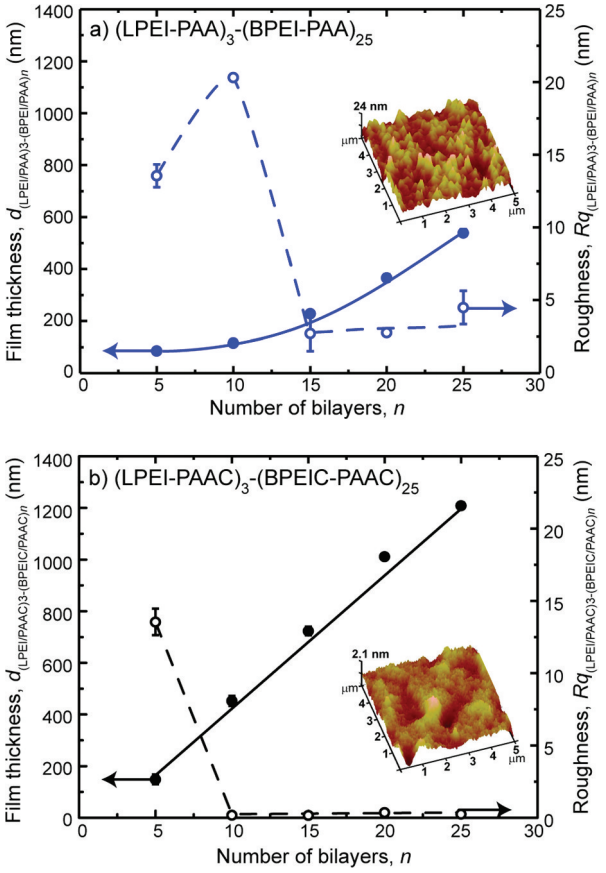

Figure 2. Growth curve and roughness of (a) $(LPEI/PAA)_3$– $(BPEI/PAA)_n$ and (b) $(LPEI/PAAC)_3$–$(BPEIC/PAAC)_n$. Height mode AFM images of $(LPEI/PAA)_3$–$(BPEI/PAA)_{25}$ and $(LPEI/PAAC)_3$–$(BPEIC/PAAC)_{25}$ are shown as inset, respectively. Note that the surface become extremely smooth in the presence of catechol-modified polyelectrolytes as the cycles are repeated.

polyelectrolyte multilayers (PEMs) (Figure 2b) grow linearly, but at different rates. It should be noted that the catechol films grow more rapidly, resulting in ~40 nm/bilayer. This increase in layer thickness may be due to an increase in the self-attractive interactions between polyion chain segments, which lead to more deposition with each adsorption step. In the case where catechol-modified polyelectrolytes were used, two nonionic types of attractions are newly introduced in addition to electrostatic interactions: hydrogen bonding interactions (e.g., between –OH in catechol groups with oxygen in –CO and/or nitrogen in $-NH_2$) and hydrophobic π–π stacking interactions (e.g., between any apposing catechol groups; see Figure 7 for details). In this case, during the deposition process, the polymer chains would be immobilized better upon adsorption because of enhanced attractive interactions with a greater number of "sticky" junctions, consequently preventing interdiffusion as shown in Figure 2b. A significant increase in surface smoothness was also observed for $(LPEI/PAAC)_3$–$(BPEIC/PAAC)_n$ films, which were prepared at constant pH and ionic strength conditions during the entire layer buildup.

To gain a better understanding of the stability of these two types of LbL films in solution, we examined their swelling behavior extensively upon immersion in PBS pH 7.4 by ex–and in–situ ellipsometry thickness measurements. Each film was examined prior to immersion, and 1 h after immersion in PBS pH 7.4, and finally the dry thickness after the swelling

dx.doi.org/10.1021/cm201801n | Chem.Mater. 2011, 23, 5349–5357

experiment was determined. When exposed to pH 7.4 buffer, the films swelled to 58.7 ± 2.5% of their dry thickness for $(LPEI/PAA)_3-(BPEI/PAA)_{25}$, and 71.2 ± 16.2% for $(LPEI/PAAC)_3-(BPEIC/PAAC)_{25}$ which are statistically similar. The changes in dry film thickness between the as-prepared films and the dry films recovered following a swelling step in PBS pH 7.4, Δd, were determined based on eq 1. Figure 3 clearly shows that

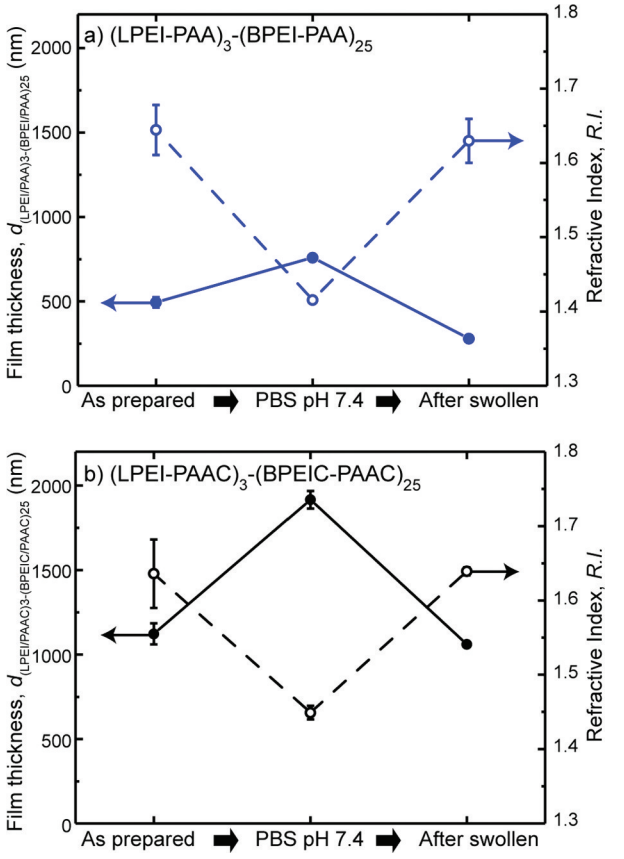

Figure 3. Changes in film thickness and refractive index of (a) $(LPEI/PAA)_3-(BPEI/PAA)_{25}$ and (b) $(LPEI/PAAC)_3-(BPEIC/PAAC)_{25}$ films. By spectroscopic ellipsometry, film thickness and refractive index values of LbL films were first measured as prepared, then during the immersion in PBS pH 7.4 and last after dried thoroughly with nitrogen gas after being swollen.

the $(LPEI/PAA)_3-(BPEI/PAA)_{25}$ film might experience some loss of polyion during the swelling process, exhibiting a clear permanent decrease in film thickness ($\Delta d < 0$, −45.0 ± 5.5% to its original dry film thickness) and visual changes in color (see Figure 4c). On the other hand, $(LPEI/PAAC)_3-(BPEIC/PAAC)_{25}$ film seemed to recover to its original thickness, resulting in $\Delta d \approx 0$ (−1.1 ± 0.5% to its original dry film thickness) and no visual changes, thereby reflecting its enhanced stability.

To establish the relationship between film stability and the charge density of the weakly charged polyelectrolytes, we determined the degree of ionization (I_{COO^-}) of PAA and PAAC in the multilayer film (n = 25) based on eq 2. To accomplish this goal, both $(LPEI/PAA)_3-(BPEI/PAA)_{25}$ and $(LPEI/PAAC)_3-(BPEIC/PAAC)_{25}$ films in the original dry state (as prepared) and dried after being swollen were carefully analyzed by FTIR spectroscopy. By estimating the relative ratio between ionized (COO^-) and nonionized (COOH) functional groups through deconvolution of spectra peaks, FTIR analysis was able to directly detect the degree of ionization (I_{COO^-}) of PAA or PAAC within the multilayer films. The FTIR measurements show that in the case of $(LPEI/PAA)_3-(BPEI/PAA)_{25}$, about 64% of carboxylic acid groups are deprotonated in the original dry films, increasing to about 75% after being exposed to the more basic pH 7.4 condition. The increase in I_{COO^-} is due to the fact that the assembly pH condition was acidic (pH 5), and therefore the carboxylic acid groups are less charged, but shift toward the COO^- state at the higher pH (pH 7.4). An increase in ionization has also been observed as an increment of I_{COO^-} from about 92 to 100% for the case of $(LPEI/PAAC)_3-(BPEIC/PAAC)_{25}$. In this second case (Figure 4b), the fraction of acid groups on the PAAC backbone that are charged are much higher during film assembly conditions of pH 5 and prior to swelling; thus, the net changes in overall fraction of protonated COOH (ΔI_{COO^-}) is much lower, and there is a complete disappearance of the COOH peak upon submersion of the film in PBS pH 7.4. Although the initial I_{COO^-} of $(LPEI/PAAC)_3-(BPEIC/PAAC)_{25}$ films appears to be higher than that of $(LPEI/PAA)_3-(BPEI/PAA)_{25}$ films, the absolute numbers of charged carboxylic acid groups per polymer chain in both films are quite similar at the same pH condition (pH 5), considering the degree of functionalization of PAAC (27.5% in this particular polymer set). In short, the PAA and PAAC polymer chains have a similar net charge density at pH 5; however, the degree to which the acid groups on these two backbones are charged is quite different. The differences in the initial degree of ionization for these two films imply that the catechol containing PAAC exhibits a lower pKa than that in the non-functionalized LbL film. A shift in pKa could be due to the presence of the phenolic catechol groups, which are more basic than the carboxylic acids and may thus serve to facilitate their deprotonation. As summarized in Figure 4c, the net result is that changes in degree of ionization (ΔI_{COO^-}) as defined in eq 2 between the as-prepared and postswelling states appear roughly two times larger in the case of the unmodified polyelectrolyte pairs. In both cases, there is also a peak at 1640 cm^{-1} that could be the primary amine N−H bend, or due to the formation of a small number of amide bonds in films.

The permanent loss of thickness, or mass, in the unmodified LbL films could be due to the out-diffusion of BPEI or LPEI upon increased pH. The pH of 7.4 is above the pKa reported for LPEI, and would be expected to yield some deprotonation of secondary and tertiary amines on LPEI and BPEI polymer backbones. The bigger ΔI_{COO^-} observed in the BPEI/PAA films could lead to further charge imbalance and destabilization of the film, leading to ejection of excess charged polyanion.[43] This loss of material results in the $\Delta d < 0$ seen in the LbL films of the unmodified polyelectrolyte pairs, as opposed to the relative stability of the catechol-modified polymer LbL films, that exhibit $\Delta d \approx 0$ and a relatively small ΔI_{COO^-} during this abrupt pH change (Figure 4c).

To ascertain the film stability in a more quantitative way, the mechanical properties of LbL films with and without catechol groups were evaluated by conducting AFM−enabled nanoindentation in PBS at pH 7.4. The inset in Figure 5 shows sets of applied force (F) vs indentation depth (δ) curves obtained from a sufficiently large number of indentation locations (at least 80), and a corresponding elastic modulus E_s calculated from eqs 3 and 4 is shown in Figure 5. At an incubation time of ∼1 h, an averaged elastic modulus E_{av} of $(LPEI/PAAC)_3-(BPEIC/PAAC)_{25}$ films was approximately five times higher than that of $(LPEI/PAA)_3-(BPEI/PAA)_{25}$ films hydrated in PBS at pH

dx.doi.org/10.1021/cm201801n | Chem.Mater. 2011, 23, 5349–5357

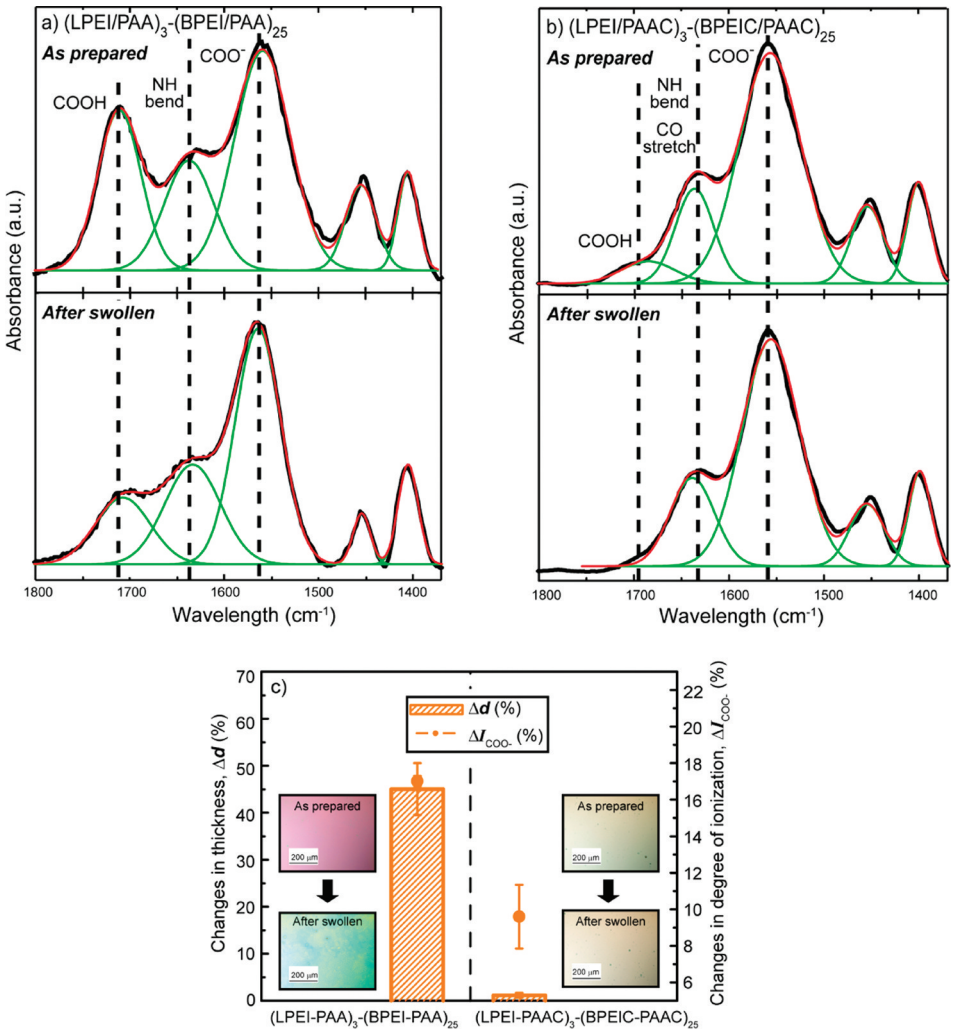

Figure 4. FTIR spectra of (a) $(LPEI/PAA)_3-(BPEI/PAA)_{25}$ and (b) $(LPEI/PAAC)_3-(BPEIC/PAAC)_{25}$ films cast from aqueous solution (as prepared) shown at the top; and dried after being immersed in PBS pH 7.4 (after swollen) at the bottom. Degree of ionization ($I_{COO}-$) of either PAA or PAAC as prepared in pH 5 and after post-treatments in pH 7.4 are determined by analyzing two spectra of COOH and COO^- peaks. The peaks at 1640 cm^{-1} are associated with the N−H bending bands in primary amine and/or in amide and C═O stretch in amide. (c) Summary of changes in films thickness (Δd) and degree of ionization ($\Delta I_{COO}-$) of $(LPEI/PAA)_3-(BPEI/PAA)_{25}$ (left side) and $(LPEI/PAAC)_3-(BPEIC/PAAC)_{25}$ (right side), along with the microscopic images of both films before (as prepared) and after swollen states. Clear color evolution was observed in $(LPEI/PAA)_3-(BPEI/PAA)_{25}$ films, while almost no visual change was detected in $(LPEI/PAAC)_3-(BPEIC/PAAC)_{25}$ films during this swelling process. Note that there are less changes in $\Delta I_{COO}-$ and Δd when catechol-modified polyelectrolytes are used. Qualitatively, the magnitude of $\Delta I_{COO}-$ moves with Δd in the same direction, strongly suggesting that the changes in degree of ionization by varying pH conditions of submerging solution would lead to rearrange polymer chains and configurations, thereby resulting in loss of materials when attractive interactions are not strong enough, as is likely the case in $(LPEI/PAA)_3-(BPEI/PAA)_{25}$ films.

7.4, indicating the enhanced mechanical stability of LbL films consisting of catechol-modified polyelectrolytes. Statistically, we observed that the elastic moduli of $(LPEI/PAAC)_3-(BPEIC/PAAC)_{25}$ films increased with time during nanoindentation measurements, resulting in a relatively broad range of stiffness distribution, presumably indicative of the ongoing oxidation of catechol groups at pH 7.4. The oxidized catechol groups could further participate in a variety of reactions, in particular, cross-linking reactions including Michael-type addition reaction, Schiff base substitution between amine and catechol groups[27] and the formation of covalent C−C and ether bonds between catechol groups.[35,36] The formation of various types of covalent bonds at pH 7.4 was detected by UV−vis absorbance spectra of films (see the Supporting Information, Figure S1). Compilation of the spectra shows a clear increase in overall absorbance, indicative of a temporal increase in the degree of covalent cross-linking in the film. To further quantify the extent of covalent cross-linking and characterize the corresponding kinetics with respect to incubation time, we determined the changes in elastic moduli of catechol-modified PEMs at different incubation times. According to the theory of rubber elasticity, the cross-linking density, ρ/M_x, is directly related to the elastic modulus by the following equation[44]:

$$E_{av} = 3\frac{\rho}{M_x}RT\nu_x^{1/3} \quad (6)$$

where R is the gas constant, T is the temperature, and v_x is the volume of film in the swollen state corresponding to the volume in dry condition at a certain incubation time, t_I. According to eq 6, the ionic cross-linking density of $(LPEI/PAA)_3-(BPEI/PAA)_{25}$ film at $t_I \approx 1$ h, purely originated from the electrostatic interactions between oppositely charged polyelectrolytes, was

dx.doi.org/10.1021/cm201801n | Chem.Mater. 2011, 23, 5349–5357

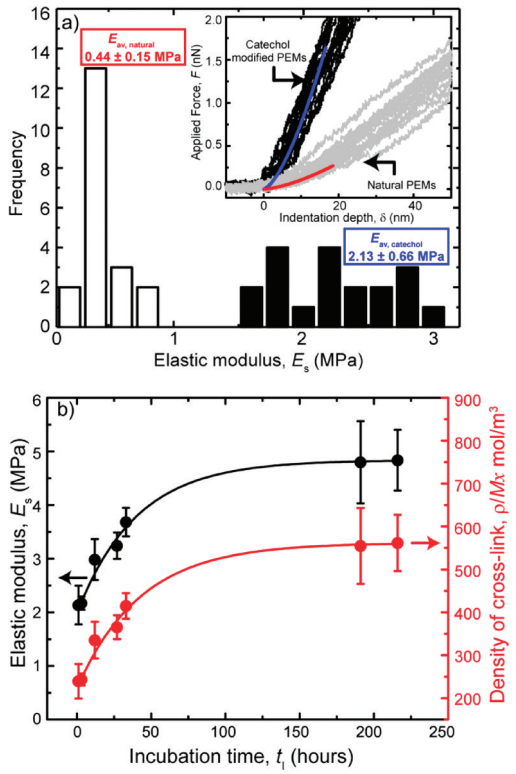

Figure 5. (a) Measured stiffness of $(LPEI/PAA)_3$–$(BPEI/PAA)_{25}$ (white columns) and $(LPEI/PAAC)_3$–$(BPEIC/PAAC)_{25}$ films (black columns) by AFM nanoindentation at $t_I \approx 1$ h. The inset shows force-depth (F–δ) responses acquired during nanoindentation of LbL films in PBS pH 7.4: $(LPEI/PAA)_3$–$(BPEI/PAA)_{25}$ (natural PEMs, solid gray); $(LPEI/PAAC)_3$–$(BPEIC/PAAC)_{25}$ (catechol-modified PEMs, solid black). The blue and red solid lines shown in the inset are representative fitting curves based on eq 3 to extract a respective elastic modulus, E_s based on eq 4. (b) Changes in measured stiffness (E_s, black circles) and effective cross-link density (ρ/M_x:, red circles) of $(LPEI/PAAC)_3$–$(BPEIC/PAAC)_{25}$ film as a function of incubation time. Both E_s and ρ/M_x followed exponential behaviors with a decay time of around 40 h and reached steady-state values within 216 h. The solid lines shown in b are fitting curves suggesting that the cross-linking process is a first-order reaction with a rate constant, $k \approx 0.023$ h^{-1}.

calculated to be 51.7 ± 17.2 mol/m^3. At the same incubation time, this value is approximately five times less than that of $(LPEI/PAAC)_3$–$(BPEIC/PAAC)_{25}$ film (239.4 ± 40.3 mol/m^3). The difference between those two values can be attributed to additional covalent cross-linking between any neighboring polyelectrolytes in the presence of catechol groups. As shown in Figure 5b, the modulus of elasticity and the cross-link density initially increased with respect to t_I but later displayed exponential plateau behavior, indicative of the termination or saturation of cross-link reactions after ~200 h (first-order reaction).

After having confirmed the improved stability of LbL films consisting of catechol-modified polyelectrolytes, we next sought to evaluate these thin films as physical barrier layers so that either a sustained or sequential release could be achieved. To do so, we first constructed two sets of films that have exactly the same base and drug layers of $(LPEI/SPS)_{10}$–$(Poly1/^{14}C\text{-}DS)_{20}$, but different physical barriers of either $(BPEI/PAA)_{25}$ or $(BPEIC/PAAC)_{25}$ films was additionally incorporated on top of the base and drug layers, as shown in Figure 6a. Figure 6a clearly shows that with unmodified $(BPEI/PAA)_{25}$ films as physical barriers, the systems release ^{14}C–DS very rapidly,

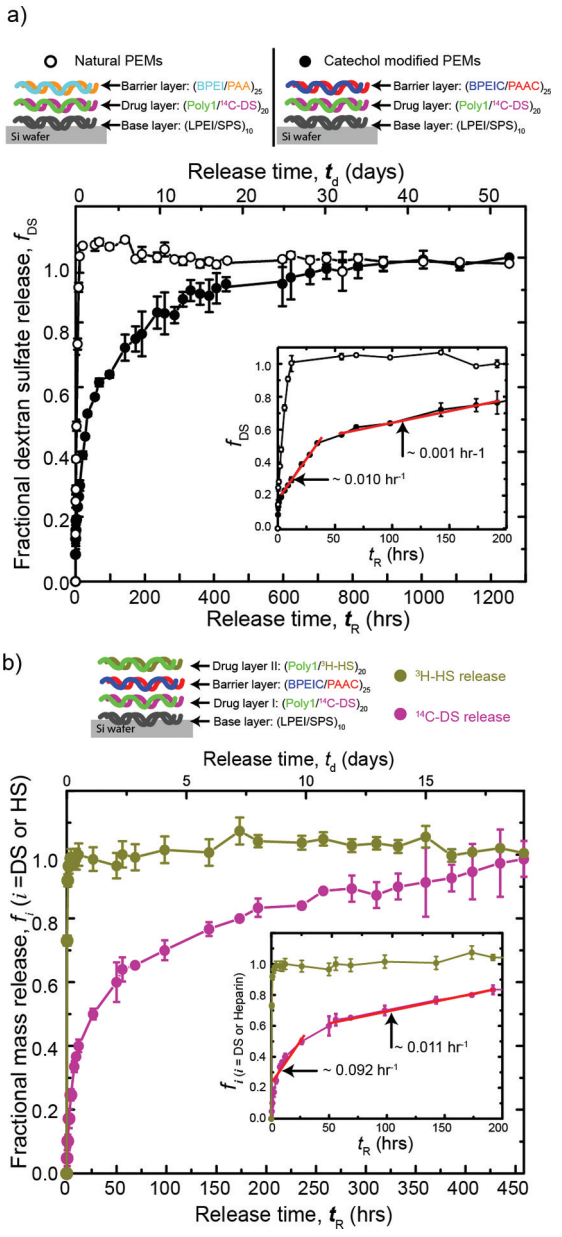

Figure 6. (a) Fractional release of radiolabeled dextran sulfate (^{14}C-DS) from $(LPEI/SPS)_{10}$–$(Poly1/^{14}C\text{-}DS)_{20}$–$(BPEIC/\ PAAC)_{25}$ films with the comparison of $(LPEI/SPS)_{10}$–$(Poly1/\ ^{14}C\text{-}DS)_{20}$–$(BPEI/PAA)_{25}$ films. During 4–50 h of incubation, the films containing catechol-modified polyelectrolytes as their physical barrier layers released over 0.089 μg/(cm^2 h) (0.010 h^{-1}), followed by a release rate of 0.011 μg/(cm^2 h) (0.001 h^{-1}) during the subsequent 200 h, and up to 40 days the films released over 0.002 μg/(cm^2 h) (0.0002 h^{-1}). (b) Fractional release of ^{14}C-DS and heparin sulfate (^{3}H-HS) from $(LPEI/SPS)_{10}$–$(Poly1/^{14}C\text{-}DS)_{20}$–$(BPEIC/PAAC)_{25}$–$(Poly1/^3H\text{-}HS)_{20}$ films. The cumulated amount of ^{14}C-DS and ^{3}H-HS released from LbL films was first normalized by the area (size) of films and later converted to the fractional release (f_{DS} or f_{HS}), which represents the fraction of released amount of ^{14}C–DS or ^{3}H–HS at a certain time point (t_R) to the final release quantity. The insets in (a) and (b) contain data from the first 200 h. Schematic architectures of three types of LbL films used for release experiments in PBS pH 7.4 at 37 °C are shown at the top of each figure, with corresponding symbols.

showing an average release rate of ~1.2 μg/(cm^2 h), which corresponds to the fractional release rate of ~0.085 h^{-1} within 12 h; after that, no further release occurred (white circles).

dx.doi.org/10.1021/cm201801n | Chem.Mater. 2011, 23, 5349–5357

On the other hand, in the presence of barrier layers consisting of catechol-modified LbL films, we observed a sustained release of ^{14}C−DS with the average release rate of 0.01 μg/(cm^2 h) and fractional release rate of ∼0.0011 h^{-1} over a period of 40 days, which strongly indicates that the catechol-modified barrier layers are capable of lengthening the release period of ^{14}C-DS (black circles in Figure 6a). This result clearly suggests that the presence of physical barriers that are purely assembled by electrostatic interactions fails to even slow the release rate, and therefore additional effects from catechol groups should be taken into account to explain the observed extended release of ^{14}C-DS. Next, the catechol-modified polyelectrolyte multilayers were further investigated as a tool to provide tunable control of the release of multiple agents. To explore the feasibility of this approach, we fabricated films using two types of radiolabeled molecules such as ^{14}C−DS and heparin sulfate (^{3}H-HS). The catechol-modified polyelectrolytes were deposited as intermediate layers between multilayers containing these radiolabeled molecules, resulting in the film architecture of $(LPEI/PAAC)_3$−$(Poly1/^{14}C\text{-}DS)_{20}$−$(BPEIC/PAAC)_{25}$−$(Poly1/^{3}H\text{-}HS)_{20}$ as shown in the schematic in Figure 6b. Figure 6b shows the results of a release experiment conducted using both ^{3}H−HS and ^{14}C−DS from the same film into solution of PBS pH 7.4 at 37 °C. In contrast to burst release profiles in which most of ^{3}H-HS is released instantly from the topmost layers of the film within less than 10 h of incubation (yellow green circles in Figure 6b), a large portion of the release of ^{14}C-DS, deposited in the bottommost layers of the film occurs in a prolonged fashion, over a period of 400 h (purple red circles in Figure 6b). The trends in release rate of ^{14}C-DS is very close to the case where no ^{3}H-HS film exists on the top of catechol-modified barrier layers as shown in Figure 6a (black circles). This result arises from the large differences in the release profiles of ^{3}H−HS and ^{14}C-DS, which are distinct and nonoverlapping after $t_R \gtrsim 10$ h, when only approximately 2% of ^{14}C-DS has been released. This result suggests that the use of catechol-modified barrier layers was sufficient to physically separate the two components and lowered interpenetration between the topmost and bottommost layers of the films during the deposition process. Considering the relatively low molecular weights (a few kDa) of ^{14}C-DS and ^{3}H-HS used in this study, it is likely that catechol-modified thin films could even further suppress the release rate of biomolecules as their size gets bigger. Because in general proteins or DNA molecules have at least one order of magnitude larger molecular weight (>a few dozen kDa) than ^{14}C-DS and ^{3}H-HS, it is expected that LbL films with catechol modifications would be more effective in sustained and sequential drug delivery applications for those biomolecules. Furthermore, it may also be possible to delay the release of smaller molecules below 1 kDa by increasing the degree of catechol modification and/or by manipulating the number of the intermediate layers without relying on harsh pretreatments using UV and/or heat.

When catechol modifications are introduced during adsorption at pH 5.0, cross-linking is relatively minimal, but the adhesive properties of mussel proteins appear in the form of two additional modes of attractive secondary interactions, such as hydrogen bond and $\pi-\pi$ stacking interactions, as shown in Figure 7. Considering the fact that hydrogen bond and $\pi-\pi$ stacking interactions occur within any adjacent catechol-modified polyelectrolytes (even among like-charged polyelectrolytes), such a modification would be beneficial for keeping the system stable against any changes in external environments, such as pH and ionic salt concentrations.

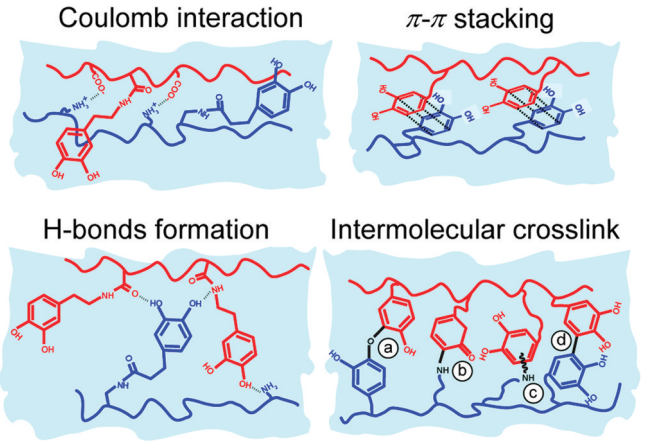

Figure 7. Schematic illustration of all possible interactions and intermolecular cross-linking reactions via. (a) Diphenyl ether formation,[35] (b) Stiff base substitution,[36,37] (c) Michael-type addition,[36,37] and (d) aryl−aryl coupling[36] in the presence of catechol groups in LbL films. Detailed discussion on the relative magnitudes of hydrogen bond interactions, $\pi-\pi$ stacking, and Coulomb interactions are given in Supporting Information, Figure S3.

The most significant change in the catechol-modified film that leads to enhanced stability is catechol polymerization, which takes place at more alkaline pH than the assembly conditions (Figure 7). Although the exact polymerization mechanism still remains unknown, it is likely that it involves oxidation of the catechol moieties when the pH of the medium is raised; after being prepared at pH 5, when the catechol groups are exposed to the aqueous medium of PBS pH 7.4 at 37 °C during release experiments, they are quickly oxidized to corresponding semiquinone or quinone forms that are highly reactive with various functional groups, including quinone itself.[27,37,45] The reactions between catechol groups[35,36] (see Figure 7a, d) and between amine and catechol groups[36,37](see Figure 7b, c) gives rise to the formation of various covalent bonds; the resultant covalent bonds create intermolecular cross-linking networks between any neighboring catechol and amine groups residing in adjacent polymer chains within LbL films. The formation of covalent bonds is likely to increase quantitatively with increased incubation time as supported by AFM nano-indentation and UV−vis absorbance measurements at PBS pH 7.4 (see Figure 5 and the Supporting Information, Figure S1).

■ CONCLUSIONS

We have introduced a facile approach to control the phenomenon of interlayer diffusion, to enhance LbL film stabilities, and to achieve a sustained release of radiolabeled biomolecules by incorporating catechol groups into polyelectrolytes. With this approach, we show that the presence of catechol groups in multilayers can recruit nonionic types of interactions (e.g., hydrogen bonding and $\pi-\pi$ stacking), and can undergo rapid cross-linking at biological pH conditions. By replacing some of the charged groups with catechol groups, such interactions are able to arise between opposite as well as like-charged polyelectrolytes, resulting in overall enhanced film stability in physiological environments. We believe that LbL films with catechol modifications are able to decrease the mixing between layers and abrupt initial burst release in PBS pH 7.4. Our study also demonstrates that three-dimensional network structures based on the covalent cross-linking process between any adjacent catechol groups at biological pH

dx.doi.org/10.1021/cm201801n | Chem.Mater. 2011, 23, 5349−5357

conditions (e.g., pH 7.4) help to further enhance mechanical properties and suppress sudden release kinetics. LbL systems with catechol modifications strongly indicate a high potential for serving as a general and efficient platform for various therapeutics, ultimately opening new venues for devising multicompartment thin films in drug delivery.

■ ASSOCIATED CONTENT

Ⓢ Supporting Information

Results of UV−vis absorbance spectra (Figure S1), FTIR spectra (Figure S2) of catechol-modified polyelectrolyte multilayers and the calculated Coulomb interaction potential for one pair of two oppositely charged ions (Figure S3) (PDF). This material is available free of charge via the Internet at http://pubs.acs.org.

■ AUTHOR INFORMATION

Corresponding Author

*E-mail: hammond@mit.edu.

■ ACKNOWLEDGMENTS

This research was supported by the U.S. Army Research Office under Contract W911NF-07-D-0004 through the Institute for Soldier Nanotechnologies at MIT. We thank Prof. Krystyn Van Vliet and Adam Zeiger for helpful discussions with AFM nanoindentation.

■ REFERENCES

(1) De Geest, B. G.; Van Camp, W.; Du Prez, F. E.; De Smedt, S. C.; Demeester, J.; Hennink, W. E. *Macromol. Rapid Commun.* **2008**, *29* (12−13), 1111−1118.
(2) De Cock, L. J.; De Koker, S.; De Geest, B. G.; Grooten, J.; Vervaet, C.; Remon, J. P.; Sukhorukov, G. B.; Antipina, M. N. *Angew. Chem., Int. Ed.* **2010**, *49* (39), 6954−6973.
(3) Such, G. K.; Quinn, J. F.; Quinn, A.; Tjipto, E.; Caruso, F. *J. Am. Chem. Soc.* **2006**, *128* (29), 9318−9319.
(4) Hammond, P. T. *Adv. Mater.* **2004**, *16* (15), 1271−1293.
(5) Decher, G. *Science* **1997**, *277* (5330), 1232−1237.
(6) Ochs, C. J.; Such, G. K.; Yan, Y.; van Koeverden, M. P.; Caruso, F. *Acs Nano* **2010**, *4* (3), 1653−1663.
(7) Such, G. K.; Johnston, A. P. R.; Caruso, F. *Chem. Soc.Rev.* **2011**, *40* (1), 19−29.
(8) Lynn, D. M. *Adv. Mater.* **2007**, *19* (23), 4118−4130.
(9) Picart, C.; Schneider, A.; Etienne, O.; Mutterer, J.; Schaaf, P.; Egles, C.; Jessel, N.; Voegel, J. C. *Adv. Funct. Mater.* **2005**, *15* (11), 1771−1780.
(10) Schneider, A.; Picart, C.; Senger, B.; Schaaf, P.; Voegel, J. C.; Frisch, B. *Langmuir* **2007**, *23* (5), 2655−2662.
(11) Richert, L.; Arntz, Y.; Schaaf, P.; Voegel, J. C.; Picart, C. *Surf. Sci.* **2004**, *570* (1−2), 13−29.
(12) Kozlovskaya, V.; Kharlampieva, E.; Mansfield, M. L.; Sukhishvili, S. A. *Chem. Mater.* **2006**, *18* (2), 328−336.
(13) Bieker, P.; Schonhoff, M. *Macromolecules* **2010**, *43* (11), 5052−5059.
(14) Picart, C.; Mutterer, J.; Richert, L.; Luo, Y.; Prestwich, G. D.; Schaaf, P.; Voegel, J. C.; Lavalle, P. *Proc.Natl. Acad. Sci. U.S.A.* **2002**, *99* (20), 12531−12535.
(15) Zacharia, N. S.; DeLongchamp, D. M.; Modestino, M.; Hammond, P. T. *Macromolecules* **2007**, *40* (5), 1598−1603.
(16) Zacharia, N. S.; Modestino, M.; Hammond, P. T. *Macromolecules* **2007**, *40* (26), 9523−9528.
(17) Harris, J. J.; DeRose, P. M.; Bruening, M. L. *J. Am. Chem. Soc.* **1999**, *121* (9), 1978−1979.
(18) Leporatti, S.; Voigt, A.; Mitlohner, R.; Sukhorukov, G.; Donath, E.; Mohwald, H. *Langmuir* **2000**, *16* (9), 4059−4063.
(19) Li, B. Y.; Haynie, D. T. *Biomacromolecules* **2004**, *5* (5), 1667−1670.
(20) Richert, L.; Boulmedais, F.; Lavalle, P.; Mutterer, J.; Ferreux, E.; Decher, G.; Schaaf, P.; Voegel, J. C.; Picart, C. *Biomacromolecules* **2004**, *5* (2), 284−294.
(21) Yang, S. Y.; Rubner, M. F. *J. Am. Chem. Soc.* **2002**, *124* (10), 2100−2101.
(22) Mendelsohn, J. D.; Barrett, C. J.; Chan, V. V.; Pal, A. J.; Mayes, A. M.; Rubner, M. F. *Langmuir* **2000**, *16* (11), 5017−5023.
(23) Mauser, T.; Dejugnat, C.; Sukhorukov, G. B. *Macromol. Rapid Commun.* **2004**, *25* (20), 1781−1785.
(24) Ibarz, G.; Dahne, L.; Donath, E.; Mohwald, H. *Adv. Mater.* **2001**, *13* (17), 1324−1327.
(25) Waite, J. H. *Integr. Comp. Biol.* **2002**, *42* (6), 1172−1180.
(26) Rzepecki, L. M.; Hansen, K. M.; Waite, J. H. *Biol. Bull.* **1992**, *183* (1), 123−137.
(27) Lee, H.; Dellatore, S. M.; Miller, W. M.; Messersmith, P. B. *Science* **2007**, *318*, 426−430.
(28) Lee, H.; Lee, Y.; Statz, A. R.; Rho, J.; Park, T. G.; Messersmith, P. B. *Adv. Mater.* **2008**, *20* (9), 1619−1623.
(29) Kang, S. M.; Rho, J.; Choi, I. S.; Messersmith, P. B.; Lee, H. *J. Am. Chem. Soc.* **2009**, *131* (37), 13224−13225.
(30) An, J. H.; Huynh, N. T.; Jeon, Y. S.; Kim, J.-H. *Polym. Int.* **2011**, DOI 10.1002/pi.3116.
(31) Ochs, C. J.; Hong, T.; Such, G. K.; Cui, J.; Postma, A.; Caruso, F. *Chem. Mater.* **2011**, *23* (13), 3141−3143.
(32) Amstad, E.; Gillich, T.; Bilecka, I.; Textor, M.; Reimhult, E. *Nano Lett.* **2009**, *9* (12), 4042−4048.
(33) Podsiadlo, P.; Liu, Z. Q.; Paterson, D.; Messersmith, P. B.; Kotov, N. A. *Adv. Mater.* **2007**, *19* (7), 949−955.
(34) Ryu, S.; Lee, Y.; Hwang, J.-W.; Hong, S.; Kim, C.; Park, T. G.; Lee, H.; Hong, S. H. *Adv. Mater.* **2011**, *23* (17), 1971−1975.
(35) Sanchez-Cortes, S.; Francioso, O.; Garcia-Ramos, J. V.; Ciavatta, C.; Gessa, C. *Colloids Surf., A* **2001**, *176* (2−3), 177−184.
(36) Pan, F. S.; Jia, H. P.; Qiao, S. Z.; Jiang, Z. Y.; Wang, J. T.; Wang, B. Y.; Zhong, Y. R. *J. Membr. Sci.* **2009**, *341* (1−2), 279−285.
(37) Lee, H.; Scherer, N. F.; Messersmith, P. B. *Proc.Natl. Acad. Sci., U.S.A.* **2006**, *103* (35), 12999−13003.
(38) Lynn, D. M.; Langer, R. *J. Am. Chem. Soc.* **2000**, *122* (44), 10761−10768.
(39) Pretsch, E.; Buhlmann, P.; Affolter, C. *Structure Determination of Organic Compounds: Tables of Spectral Data*, 3rd ed.; Springer: New York, 2000; p 395.
(40) Choi, J.; Rubner, M. F. *Macromolecules* **2005**, *38* (1), 116−124.
(41) Xie, A. F.; Granick, S. *Macromolecules* **2002**, *35* (5), 1805−1813.
(42) Dimitriadis, E. K.; Horkay, F.; Maresca, J.; Kachar, B.; Chadwick, R. S. *Biophys. J.* **2002**, *82* (5), 2798−2810.
(43) Kharlampieva, E.; Ankner, J. F.; Rubinstein, M.; Sukhishvili, S. A. *Phys. Rev. Lett.* **2008**, *100*, 12.
(44) Treloar, L. R. G. *Physics of Rubber Elasticity*; Monographs on the Physics and Chemistry of Materials; Clarendon Press: Oxford, U.K., 1958; Vol. 2nd ed.; p 193.
(45) LaVoie, M. J.; Ostaszewski, B. L.; Weihofen, A.; Schlossmacher, M. G.; Selkoe, D. J. *Nat. Med.* **2005**, *11* (11), 1214−1221.